The Mechanisms of Summer Dryness Induced by Greenhouse Warming

R. T. WETHERALD AND S. MANABE

Geophysical Fluid Dynamics Laboratory/NOAA, Princeton University, Princeton, New Jersey

(Manuscript received 7 February 1995, in final form 24 May 1995)

ABSTRACT

To improve understanding of the mechanisms responsible for CO_2-induced, midcontinental summer dryness obtained by earlier modeling studies, several integrations were performed using a GCM with idealized geography. The simulated reduction of soil moisture in middle latitudes begins in late spring and is caused by the excess of evaporation over precipitation. The increase of carbon dioxide and the associated increase of atmospheric water vapor enhances the downward flux of terrestrial radiation at the continental surface at all latitudes. However, due mainly to the CO_2-induced change in midtropospheric relative humidity, the increase in the downward flux of terrestrial radiation is larger in the equatorward side of the rain belt, making more energy available there for both sensible and latent heat. Since the saturation vapor pressure at the surface increases nonlinearly with surface temperature, a greater fraction of the additional radiative energy is realized as latent heat flux at the expense of sensible heat. Therefore, evaporation increases more than precipitation over the land surface in the equatorward side of the rain belt during spring and early summer and initiates the drying of the soil there. As the rain belt moves poleward from spring to summer, the soil moisture decreases in middle latitudes, reducing the rate of evaporation. This reduction of evaporation, in turn, causes a corresponding decrease of precipitation in middle latitudes, keeping the soil dry throughout the summer.

In high latitudes, there is also a tendency for increased summer dryness. As noted in our previous studies, this feature mainly results from the earlier removal of highly reflective snow cover in spring, which enhances the evaporation in the late spring, lengthening the period of drying during the summer season. A similar mechanism also operates in middle latitudes, but its contribution is relatively small. The drying of soil is also enhanced by the land surface–cloud interaction in both middle and high latitudes. Owing to the reduction of cloud cover that results from the decrease of relative humidity in the lower troposphere, solar radiation absorbed by the continental surface increases, thereby enhancing evaporation and further reducing the soil moisture in summer.

Although there is additional radiative energy available at the surface during winter, a greater fraction of it occurs as sensible heat rather than latent heat due to the colder surface temperature, thereby causing evaporation to increase less than precipitation. Because of the increased evaporation from the oceanic surface upstream whose temperature is warmer than the continental region in winter, precipitation over most of the continent increases substantially.

1. Introduction

The effect of an increase of atmospheric carbon dioxide upon soil wetness has been the subject of several past investigations conducted at the Geophysical Fluid Dynamics Laboratory (Manabe et al. 1981; Manabe and Wetherald 1985, 1987). Among other features, these studies identified a distinct tendency for soil moisture to be substantially reduced during the summer over extensive continental regions in middle latitudes. Although there was considerable variation of summertime soil moisture changes in comparable studies conducted outside of GFDL (Mitchell and Warrilow 1987; Kellogg and Zhao 1988), this feature has been reproduced, in general, by more recent investigations utilizing higher-resolution models, which are summarized in Mitchell et al. (1990).

In past GFDL studies, this summer dryness in middle latitudes was ascribed to an earlier termination of the spring rainy season due to a poleward shift of the middle latitude rain belt and an earlier snowmelt season, both of which resulted in a longer and warmer drying season. The poleward shift of the rain belt was attributed to the penetration of moisture-rich air into higher latitudes. Summer dryness was also enhanced by a reduction of cloud cover, which increased insolation and evaporation at the model surface. However, it was discovered in subsequent integrations that the poleward shift of the middle-latitude rain belt sometimes occurred only during the summer season, suggesting that this feature may be a result rather than a cause of the middle-latitude summer dryness. Also, this poleward shift of the middle-latitude rain belt is not accompanied by a similar poleward shift of the middle-latitude jet stream. Therefore, the main objective of the current study is to conduct an in-depth analysis of the physical

Corresponding author address: Dr. Richard T. Wetherald, GFDL/NOAA, Princeton University, P.O. Box 308, Princeton, NJ 08542.
E-mail: rw@gfdl.gov

processes involved in the initiation and maintenance of continental summer dryness.

Because the middle-latitude rain belt is often obscure in GCMs utilizing irregular geography, we decided to use a GCM with idealized geography and without mountains in order to facilitate the analysis of the various interactions or feedback mechanisms involved. In particular, we will attempt to answer the following three questions: 1) what is the role of the interaction of soil moisture with the surface hydrologic processes in inducing summer dryness in middle latitudes, 2) what role does snow cover and its disappearance in spring play in determining summer dryness at both middle and high latitudes, and 3) what role does cloud cover change play in determining the overall degree of summer dryness?

2. Model description

The model used here is similar to models used in previous GFDL climate investigations. The version of the model employed for this study consists of three parts: 1) a mathematical model of the atmosphere using the spectral method, 2) a heat and water balance over the continents, and 3) a simple mixed layer of the ocean with a uniform depth of 50 m. The dynamical component of the atmospheric model is similar to that described by Gordon and Stern (1982) except that the realistic geography is replaced by a "sector" domain consisting of three identical sectors of equal flat land and sea bounded by meridians that are 120 degrees of longitude apart (see Fig. 1). The spectral computation employs the "rhomboidal 15" wavenumber truncation in which 15 associated Legrendre functions are retained for each of the 15 Fourier components. Vertical derivatives in the prognostic equations are computed by a centered, second-order finite difference with nine unequally spaced levels.

The distribution of insolation at the top of the model atmosphere is prescribed seasonally but has no diurnal cycle. The mixing ratio of carbon dioxide is assumed to be constant everywhere (300 ppm), whereas the zonally uniform ozone is specified as a function of latitude, height, and season. Cloud cover is predicted, essentially, according to the scheme of (Wetherald and Manabe 1988). Overcast cloud is placed whenever the relative humidity is equal to or exceeds the critical value of 99%. This critical value was chosen such that the global mean values of cloud amount and its thermal forcing are realistic. However, the cloud optical properties for solar radiation are prescribed separately for high, middle, low, and thick cloud as functions of the zenith angle instead of the constant values used previously. All clouds, including high cloud, are assumed to be black bodies.

Over the continents, surface temperature is computed from the condition of heat balance at the surface under the assumption of zero heat capacity. This heat balance consists of incoming solar radiation, net outgoing longwave radiation, sensible heat, and latent heat plus snowmelt.

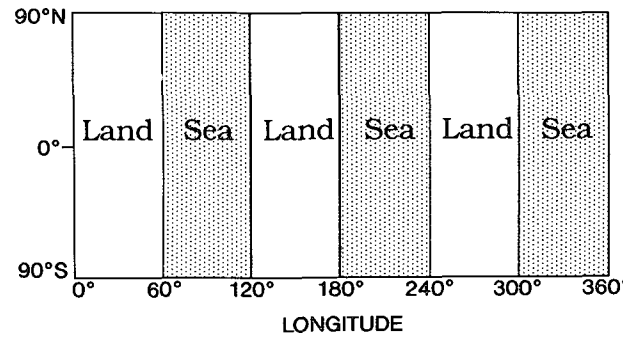

FIG. 1. Computational domain of the model.

Precipitation is predicted whenever supersaturation is present in the model and occurs in convective and nonconvective forms according to the scheme described in Manabe et al. (1965). Distinction is made between rainfall and snowfall depending upon whether the temperature of the air just above the surface is above or below freezing, respectively.

The moisture-holding capacity of soil is represented by a single 15-cm "bucket," which is either replenished by rainfall and snowmelt or depleted by evaporation and runoff. Continental evaporation is assumed to be a function of the soil moisture and potential evaporation rate (i.e., the hypothetical evaporation rate from a completely wet surface). Runoff is calculated as the excess of moisture input only when the bucket is full. Refer to Manabe (1969) for more details on the hydrology of the continental surface.

The oceanic mixed layer model consists of a vertically isothermal layer of water with a uniform depth of 50 m. Over ice-free regions, the rate of change of the mixed layer temperature with time is computed from the net balance of solar and terrestrial radiative fluxes and sensible and latent heat fluxes at the ocean surface. For regions covered by sea ice, the mixed layer temperature is fixed at the freezing point of sea water and the heat conduction through the ice is balanced by the latent heat of freezing (melting) at the bottom of the ice layer. This process, together with melting at the ice surface, sublimation, and snowfall, determines the change in the ice thickness (Bryan 1969).

The albedo of snow cover depends upon surface temperature and snow depth (Manabe et al. 1991). For deep snow (water equivalent of at least 2 cm), the surface albedo is 60% if the surface temperature is below −10°C and 45% at 0°C with a linear interpolation between these two values from −10° to 0°C. When the water equivalent of the snow depth is less than 2 cm, it is assumed that the albedo decreases from the deep snow values to the albedo of the underlying surface as a square root function of snow depth. The albedo of sea ice is prescribed in a sim-

ilar manner. In this case, the limits are for thick ice (at least 1 m thick) 80% if the surface temperature is below −10°C, 55% at 0°C, and linearly interpolated between these two values for intermediate temperatures. Finally, as in the land case, the albedo decreases as a square root function of sea ice thickness from the thick ice values to the value of open ocean if the thickness falls below 1 cm. For snow-free land or ice-free ocean, the surface albedo is prescribed geographically, based upon the study by Posey and Clapp (1964).

3. Design of experiment

To identify and explore the possible mechanisms responsible for the CO_2-induced summer dryness, we decided to evaluate the various interactions involving soil moisture, snow cover, and cloud cover. The perturbation chosen for this investigation is a quadrupling rather than a doubling of atmospheric CO_2 to increase the "signal-to-noise ratio" between the CO_2-induced change and the natural fluctuation of the model climate. Here, the response of a model climate to the quadrupling of CO_2 was computed by subtracting the equilibrium climate with the standard CO_2 concentration of 300 ppm (1×) from the climate with four times the standard concentration (4×).

Four different versions of the model were constructed. The special characteristics of each version are outlined in Table 1. Each version was integrated for both values of CO_2 for a period of 30 model years. In each case, the first 20 years were required to reach climatic equilibrium. The last 10 years of each integration were, then, averaged to remove the natural variability of the model climate and to produce the time-mean data for analysis. In addition, because the land–sea distributions of the two hemispheres of the model are identical (Fig. 1), the annual marches of the hydrological variables from the two hemispheres are averaged to increase the statistical sample size. For each version of the model, the equilibrium climates from both the 1× and 4× integrations were obtained in order to evaluate the response to the quadrupling of atmospheric CO_2. Initial conditions consisted of a resting, isothermal atmosphere for all cases.

The first version is the basic general circulation model described in the preceding section with no additional modification. This version serves as the standard or "control" experiment to which all other experiments will be compared and is denoted, hereafter, as the fully interactive experiment FI.

The second version of the model is constructed to evaluate the effect of removing soil moisture feedback from the model. In this version, the seasonal and geographical distribution of soil moisture is prescribed (rather than predicted) for both the 1× and 4× integrations, thereby removing the soil moisture anomalies from the model. The prescribed distribution is obtained from the 1× integration of FI as monthly mean fields for the 12 months and linearly interpolated from one month to another to produce the required daily values. Since an identical distribution of soil moisture is prescribed in both the 1× and 4× integrations, the response of the model climate obtained from this experiment is not affected by the soil moisture feedback. This version of the model will, hereafter, be denoted as the prescribed soil moisture experiment PW.

TABLE 1. Identification of the various experiments performed.

ID	Name	Characteristics
FI	fully interactive (control)	all feedbacks included
PW	prescribed soil moisture	no soil moisture feedback
PS	prescribed snow cover	no snow/albedo feedback
PC	prescribed cloud cover	no cloud cover feedback

The third version of the model was created to evaluate the effect of eliminating snow cover feedback from the model. In this version, it is assumed that all precipitation occurs as rainfall irrespective of atmospheric temperature. Thus, the computations of the snow budget and its effect on the changes of snow cover and surface albedo are absent. In other words, both the snowdepth and snowmelt are maintained at zero everywhere. To account for the thermal effect of the normal snow cover, we replaced the snow cover–dependent albedo computation with a prescribed distribution of the surface albedo. The prescribed albedo is obtained from the 1× integration of FI as monthly mean fields for the 12 months and linearly interpolated from one month to another to produce the required daily values. This prescribed distribution of surface albedo was, then, applied to both the 1× and 4× integrations, thereby removing the contribution of the snow cover feedback process from the model response to the quadrupling of CO_2. This version of the model will, hereafter, be referred to as the prescribed snow cover experiment PS.

The fourth, and final, version of the model was designed to evaluate the effect of eliminating cloud feedback from the model. In this version, we replaced the cloud cover computation with a prescribed cloud cover. The prescribed cloud cover consisted of the daily cloud distributions obtained from the 1× integration of FI over one annual cycle, which were then used directly without interpolation. This prescribed distribution of cloud cover was, then, applied to both the 1× and 4× integrations of this experiment, thereby eliminating the cloud feedback process from the model. This fourth version will, hereafter, be denoted as the prescribed cloud cover experiment PC.

The basic strategy of this study will be to compare the results obtained from the three cases (PW, PS, and PC), respectively, to the control case FI in order to evaluate, separately, the relative importance of each mechanism given above. In other words, to evaluate the effect of soil moisture feedback, the equilibrium response of PW is compared with that obtained from

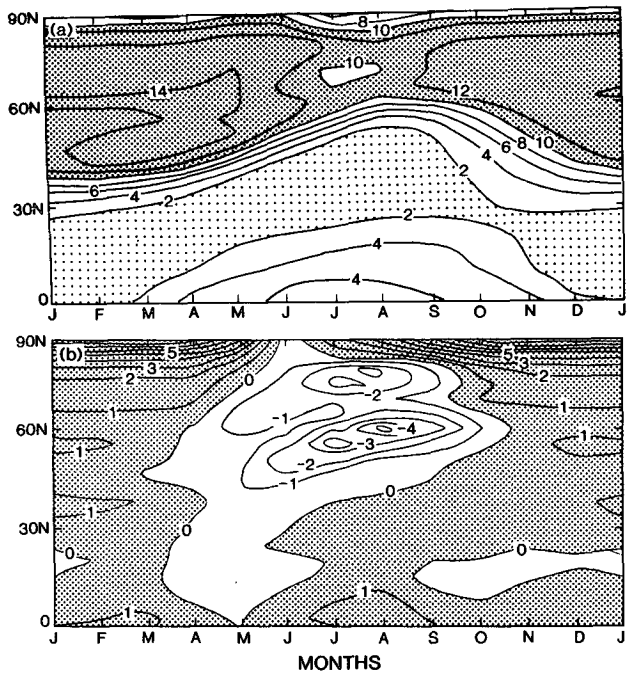

FIG. 2. Latitude–month distributions of zonally averaged, monthly mean (a) soil moisture and (b) difference of soil moisture between the 4× and 1× integrations obtained from the FI experiment. Units are in cm.

FI; to evaluate the effect of snow cover feedback, the equilibrium response of PS is compared to that of FI, and, finally, to evaluate the effect of cloud feedback, the equilibrium response of PC is compared to that of FI. In all of the results presented in this paper, the distributions of the two hemispheres of the model are averaged together over all three land sectors after shifting the phase of the Southern Hemisphere variation by six months. In the following discussions, the terms "middle latitudes" and "high latitudes" refer to 45°–60° and 70°–80° lat, respectively.

4. Hydrologic response

a. The fully interactive experiment

Our analysis of summer dryness starts with a brief discussion of the fully interactive experiment FI and its relationship to the previous GFDL studies. Figure 2 shows the seasonal variation of zonally averaged, monthly mean soil moisture and its CO_2-induced change obtained from FI. As Fig. 2a indicates, the boundary of the region of relatively large soil moisture shifts poleward in spring and equatorward in fall following the movement of the middle-latitude rain belt. In response to the increase of atmospheric CO_2, soil moisture reduces in middle latitudes during late spring and throughout the entire summer season into early fall (Fig. 2b). A secondary zone of soil moisture reduction during the summer is also apparent in higher latitudes. Qualitatively similar results have been obtained from a number of earlier GFDL studies (Manabe et al. 1981; Manabe and Wetherald 1985, 1987). A reverse ten-

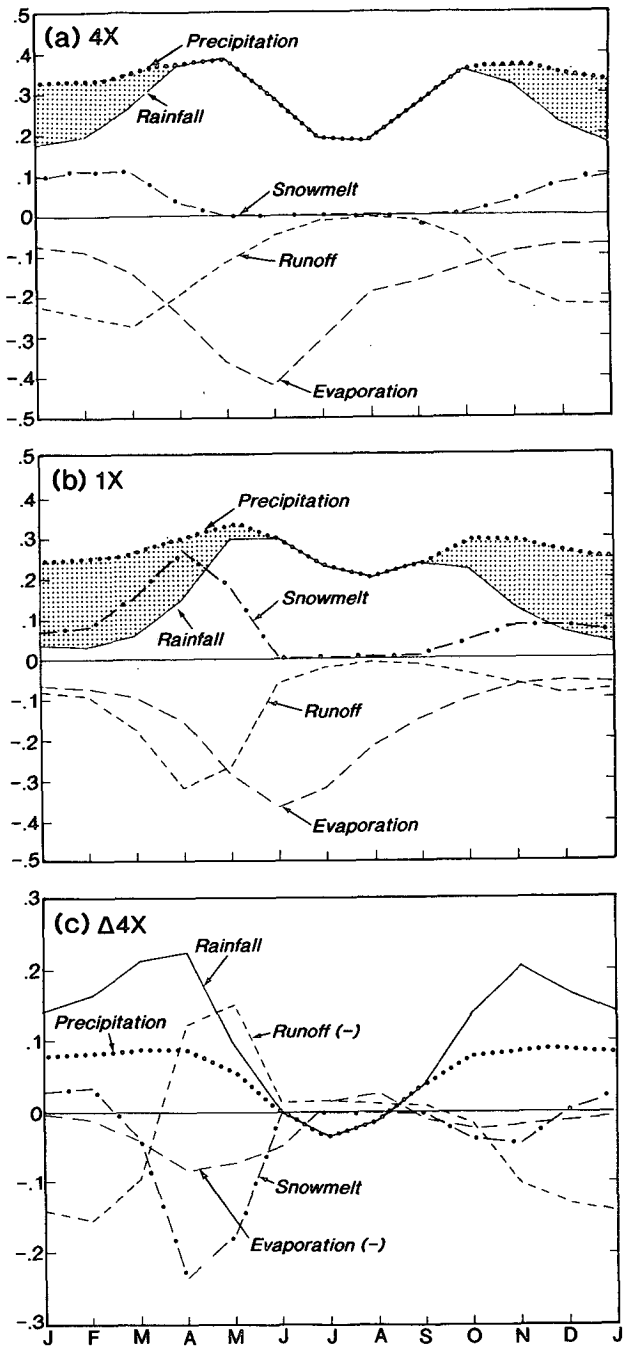

FIG. 3. Seasonal variation of the monthly mean surface water budget averaged over the continental region of 45°–60° lat for the FI experiment. (a) The 4× integration, (b) the 1× integration, and (c) the difference between the 4× and 1× integrations. Shaded regions in both (a) and (b) denote portion of precipitation (dotted line) attributable to snowfall. Units are in cm day^{-1}.

dency is observed during the winter and early spring seasons in middle latitudes where soil moisture actually increases in response to the greenhouse warming.

Figure 3 illustrates the seasonal variations of the middle-latitude surface water budget components for both the 1× and 4× integrations of the FI experiment and their differences. For the 4× integration of FI, this figure shows an earlier onset of increased rainfall and evaporation as well as an earlier melting of snow cover during spring followed by slightly decreased rainfall and evaporation during summer. However, this earlier onset of the spring rainfall is caused, simply, by a decreased fraction of total precipitation attributable to snowfall as compared with the 1× integration (see shaded regions of Fig. 3a,b). On the other hand, total precipitation increases rather uniformly throughout the winter and spring seasons before decreasing during the summer months. Although the increase of evaporation during spring in middle latitudes has been partially attributed in past studies to an earlier removal of snow cover there, it will be shown in a later section that this mechanism plays a relatively minor role in causing the subsequent decrease in soil moisture during summer. Also, since the soil is nearly saturated during the early spring season in middle latitudes, most of the earlier snowmelt and additional rainfall in the 4× integration occurs as runoff rather than increasing the soil moisture. In any event, the CO_2-induced drying in middle latitudes is initiated in the equatorward side of the middle latitude rain belt during late spring when the CO_2-induced increase of evaporation is larger than that of precipitation, followed by a drier summer with reduced precipitation and evaporation (Fig. 3c).

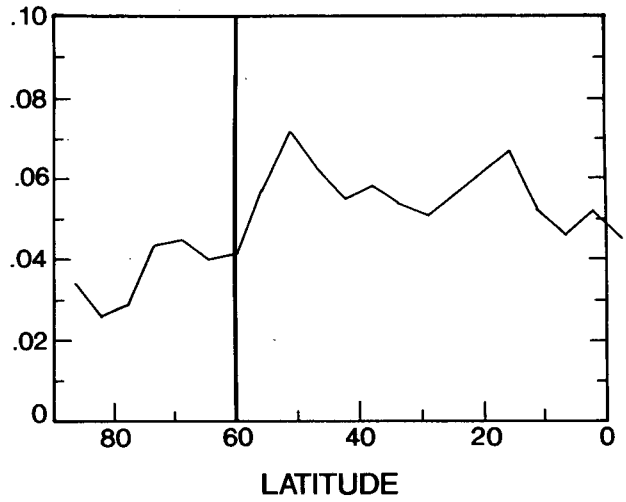

FIG. 4. Latitudinal distribution of zonal mean difference of evaporation rate, over the continent, between the 4× and 1× integrations of the PW experiment averaged for the summer months June–August. The vertical solid line at 60° lat indicates the mean position of the middle-latitude rain belt for the same time period. Units are in cm day^{-1}.

b. Soil moisture interaction

In the preceding section, it is suggested that, in the FI experiment, the CO_2-induced, midcontinental reduction of soil moisture in summer results mainly from the changes in evaporation and precipitation during late spring and summer. On the other hand, these changes, in turn, are strongly influenced by the summer reduction of soil moisture mentioned above. To elucidate the land surface–atmosphere interaction involved, an analysis was performed on the seasonal variation of surface budgets of heat and water obtained from not only the FI experiment but also the PW experiment in which the distribution of soil moisture is prescribed and does not change from the 1× to the 4× integrations.

Figure 4 illustrates, for the PW experiment, the latitudinal profile of the CO_2-induced change in evaporation rate averaged over the three summer months of June through August. It indicates that the evaporation rate increases more on the equatorial side of the middle latitude rain belt than it does on the poleward side. To examine this asymmetric change in evaporation, we illustrate in Fig. 5, the latitudinal profiles of the changes of various surface heat budget components. Owing mainly to the increase of carbon dioxide and water vapor in the model atmosphere, the CO_2-induced change in net downward longwave radiation is positive on both sides of the rain belt. However, because the midtropospheric relative humidity is reduced in the middle-latitude rain belt and increases slightly in the subtropics in response to the quadrupling of CO_2 (Fig. 6), the CO_2-induced increase in the downward flux of terrestrial radiation increases from 60° to 30° lat (Fig. 5a). Thus, the increase in the net downward flux of radiation is greater in the equatorward portion of the middle-latitude rain belt, making more energy available there for both sensible and latent heat fluxes (Fig. 5b). Also, since the saturation vapor pressure at the surface increases nonlinearly with surface temperature, a greater fraction of the additional radiative energy is realized as latent heat at the expense of sensible heat. Therefore, the CO_2-induced increase in evaporation is larger in the equatorward than the poleward side of the rain belt (Fig. 5b).

Because continental wetness is determined by the difference between precipitation and evaporation ($P-E$), it is necessary to examine the latitudinal distribution of the CO_2-induced change of this quantity obtained from the PW experiment as illustrated in Fig. 7. This figure shows a latitudinal zone of $P-E$ decrease in the equatorward portion of the middle-latitude rain belt during the summer season, resulting in the reduction of soil moisture there. On the other hand, ($P-E$) has a relatively small increase on the poleward side. Figure 8b illustrates the annual march of the CO_2-induced changes of precipitation and evaporation in middle latitudes for PW. It reveals that evaporation in-

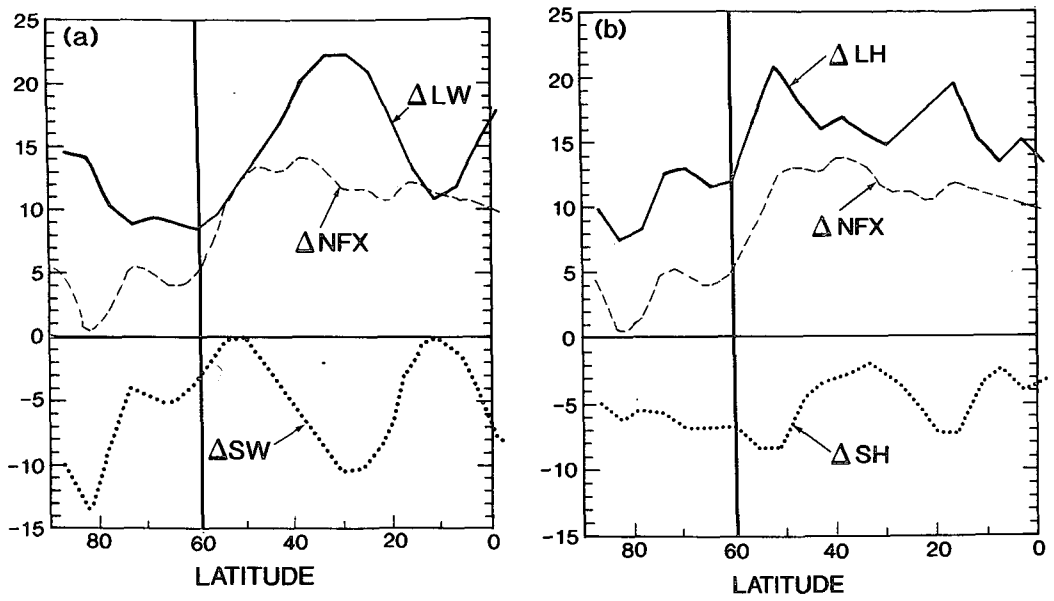

FIG. 5. Latitudinal distributions, over the continents, of zonal mean differences in fluxes of (a) net radiation (NFX), net solar radiation (SW), and net longwave radiation (LW) and; (b) net radiation (NFX), latent heat flux (LH), and sensible heat flux (SH) between the 4× and 1× integrations of the PW experiment averaged for the summer months June–August. The vertical solid line at 60° lat for both (a) and (b) indicates the mean position of the middle-latitude rain belt for the same time period. Units are W m^{-2}.

creases more than precipitation over the land surface when the surface temperature becomes high during the warm season beginning as early as May. Because of the increase in evaporation from both the continental and oceanic surfaces, precipitation also increases. However, in this experiment, evaporation increases are greater than the simultaneous increase of precipitation during the warm summer over the midlatitude continents where evaporation is greater than precipitation (Fig. 8a). Since moisture is prescribed in this experiment, this tendency continues throughout the entire summer season. These results lead to the conclusion that drying would have occurred in the equatorward portion of the middle-latitude rain belt (45°–60° lat) during the entire summer season in the PW experiment if the soil moisture had not been prescribed.

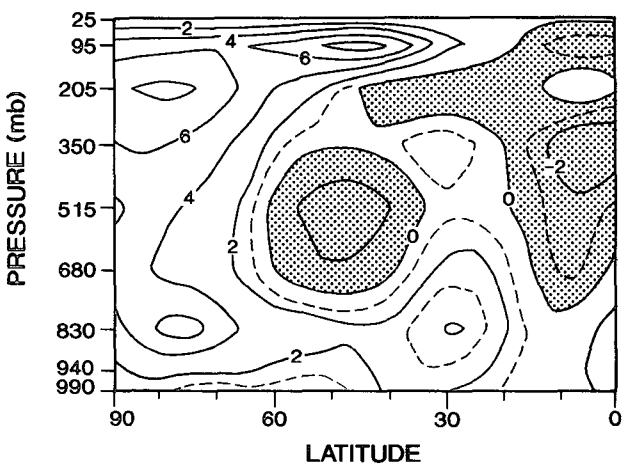

FIG. 6. Latitude–height distribution of zonal mean difference of relative humidity, over the continent, between the 4× and 1× integrations of the PW experiment averaged for the months of June–August. Units are in percent.

In the FI experiment, the increase of evaporation during spring is, again, initiated by the net increase of radiative energy at the surface. As Fig. 9a indicates, evaporation increases during the entire spring for FI just as it did for PW until July when the soil becomes too dry to support an increased amount of evaporation. Subsequently, evaporation is reduced in the equatorward side of the rain belt during July and August. This reduction of evaporation, together with the reduction of soil moisture from May to June (Fig. 9b), results in a decrease of precipitation in the equatorward portion of the rain belt during most of the summer season as Fig. 9a (solid line) shows. The decrease of precipitation there for FI, then, causes a poleward shift of the middle-latitude rain belt throughout the summer season, which is shown in Fig. 10a. In other words, the poleward shift of the middle-latitude rain belt during summer is a direct result of soil moisture change. Therefore, the reduction of middle-latitude soil moisture is initiated in May when the increase of evaporation exceeds that of precipitation and continues through June. At this point,

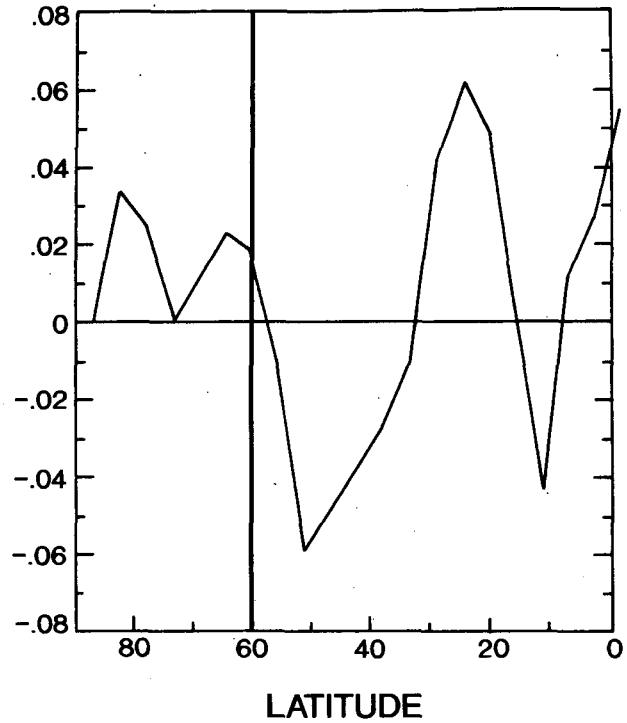

FIG. 7. Latitudinal distribution of zonal mean difference of precipitation minus evaporation ($P-E$) rate, over the continent, between the 4× and 1× integrations of the PW experiment averaged over the months of June to August. Units are in cm day^{-1}.

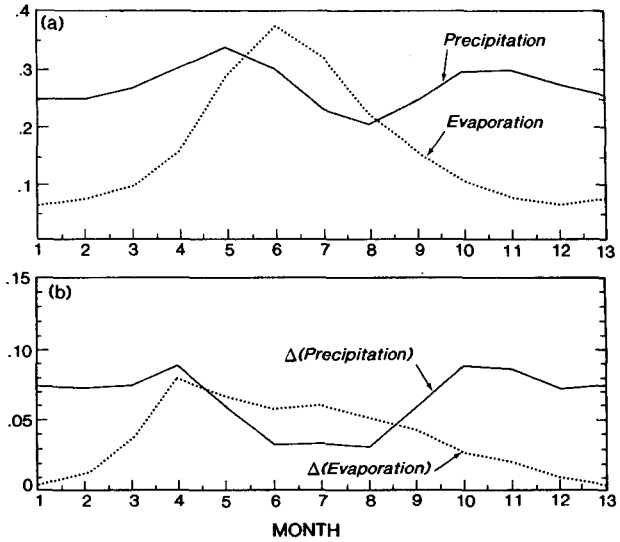

FIG. 8. Seasonal variation of monthly mean rates of (a) evaporation and precipitation for the 1× integration of PW and (b) their differences between the 4× and 1× integrations of PW averaged over the continental region of 45° to 60° lat. Units are in cm day^{-1}.

the decrease of precipitation due to soil moisture reduction takes over and keeps the soil moisture depleted throughout the rest of the summer (Fig. 9a,b). A similar excess of the CO_2-induced change in evaporation over precipitation takes place for PW during May and June in middle latitudes, which continues throughout the entire summer because of the prescribed soil moisture condition (Fig. 8b). Because the soil moisture anomalies affecting evaporation are absent in the PW experiment, the poleward shift of the middle-latitude rain belt is not as evident for this experiment as it is for FI (Fig. 10b).

The change of soil moisture described above also affects the CO_2-induced increase of surface temperature. In the case of PW, the increase of surface absorption of downward radiative flux accounts for the increased latent heat flux throughout the entire summer season in middle latitudes (Fig. 11a). On the other hand, for FI, increased sensible heat flux resulting from the increased surface–air temperature difference is mainly responsible for removing the increased radiative heat energy absorbed by the surface as the soil becomes drier during summer (Fig. 11b). Thus, the surface temperature increases more over the continent in middle latitudes during summer in FI as compared with PW (Fig. 12a,b).

During the winter season, the CO_2-induced changes of surface heat and hydrologic components are quite different from those during summer for both the FI and PW experiments. Since the saturation vapor pressure increases nonlinearly with increasing temperature, the CO_2-induced increase in evaporation is much less over the cold continental surface in winter than in summer.

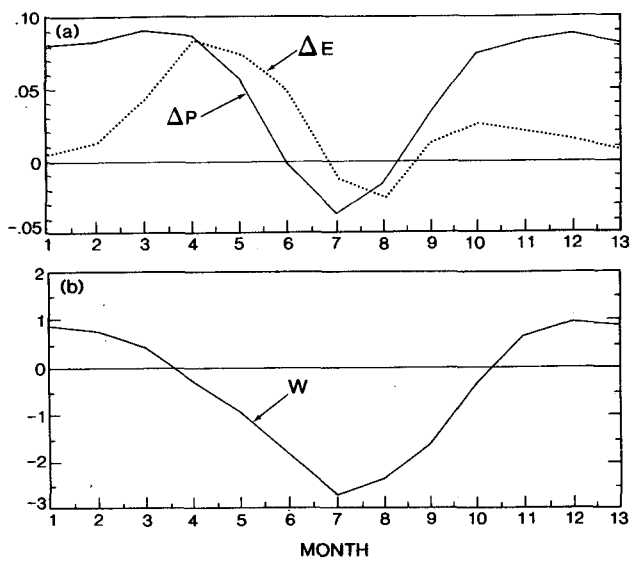

FIG. 9. Seasonal variation of the monthly mean difference between the 4× and 1× integrations of (a) evaporation and precipitation rates and (b) soil moisture averaged over the continental region of 45° to 60° lat for the FI experiment. Units are cm day^{-1} for (a) and cm for (b), respectively.

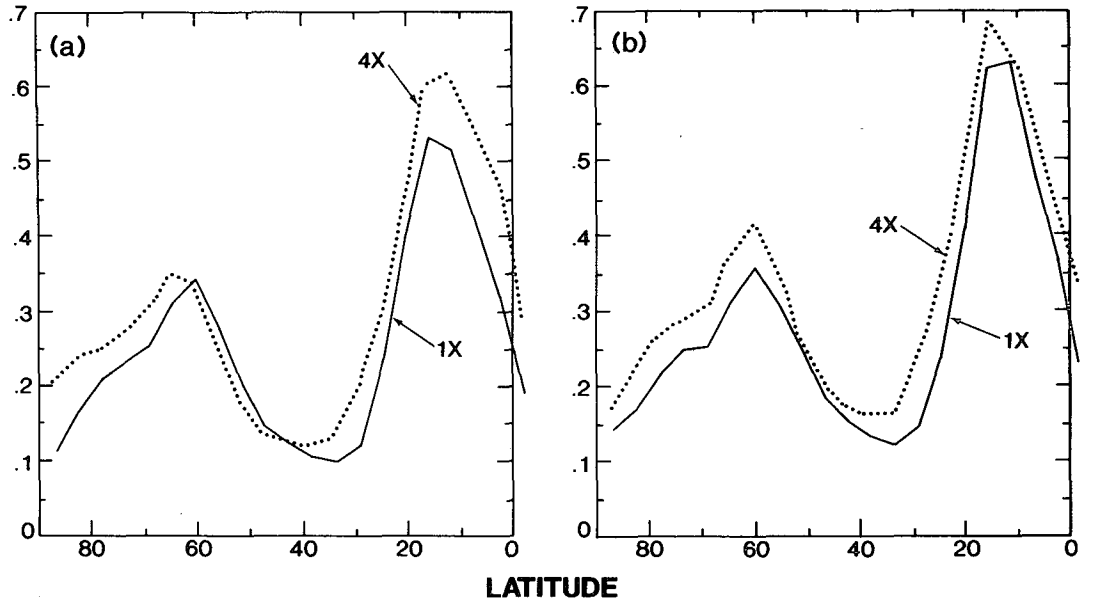

FIG. 10. Latitudinal distribution of zonal mean precipitation rate, over the continent, averaged for the summer months June–August for both the 4× and 1× integrations of the (a) FI and (b) PW experiments. Units are in cm day^{-1}.

Therefore, although additional radiative energy is available at the surface due to the increased CO_2 and water vapor in the atmosphere, a greater amount of this energy is realized as sensible heat rather than latent heat in winter (Fig. 11a,b). Thus, evaporation increases less than precipitation, thereby contributing to an increase of soil moisture. Precipitation over the continents is enhanced by increased evaporation from the ocean upstream where the temperature is higher than the adjacent continental region during the winter season and the increased radiative energy available at the surface is removed more in the form of latent than sensible heat flux in winter. This is in contrast to the situation in summer when the surface temperature over the ocean tends to be lower than over the continents and the increase in evaporation from the wet continent is often greater than over the ocean at comparable latitudes. One should note, however, that the increase in soil moisture is limited in winter because the soil is nearly saturated with water (Fig. 2a) and most of the additional moisture in both experiments occurs as runoff. The importance of this latter feature is discussed in Mitchell and Warrilow (1987).

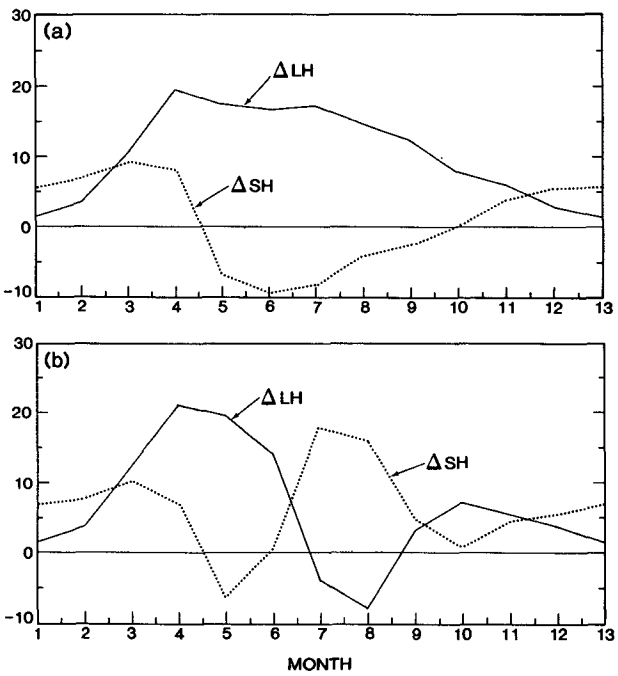

FIG. 11. Seasonal variation of the monthly mean differences of both the latent and sensible heat fluxes between the 4× and 1× integrations for the (a) PW experiment and (b) FI experiment averaged over the continental region of 45°–60° lat. Units are in W m^{-2}.

5. Snow cover feedback analysis

In Fig. 2b of section 4, one notes that a decrease of soil moisture also occurs during the summer in high latitudes (70°–80° lat) for FI. To investigate this feature, we will now consider the case in which the snow albedo feedback process is absent (PS). Figure 13 shows the CO_2-induced change of soil moisture for PS (Fig. 13a) and the difference of soil moisture change between the FI and PS experiments (Fig. 13b). According to Figs. 2b and 13a,b, the reduction of soil moisture in high latitudes obtained from FI is much

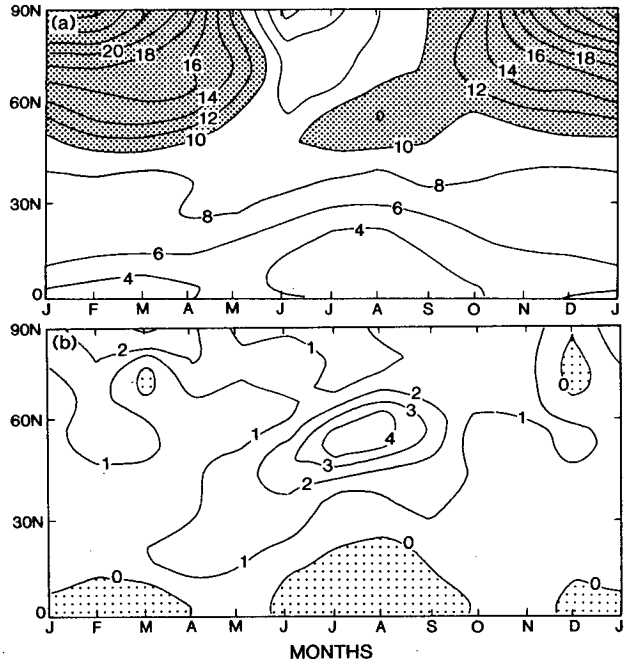

FIG. 12. Latitude–month distributions of zonally averaged, monthly mean difference of surface air temperature, over the continent, between the 4× and 1× integrations obtained from the (a) FI experiment and (b) the difference between the FI and PW experiments. Units are in °C.

greater than that derived from PS. This suggests that the effects of the earlier disappearance of snow cover followed by enhanced evaporation accounts for more than half of the change of soil moisture there in the FI experiment.

To substantiate this conclusion, we examined the changes of the surface heat and water budgets at high latitudes for both FI and PS. According to our analysis of FI, snow cover melts and disappears earlier due to the increased downward flux of terrestrial radiation, which results from the additional CO_2 and water vapor. This, in turn, causes both an earlier beginning and ending of the water supply through snowmelt and the earlier removal of highly reflective snow cover during spring. Since the soil moisture in high latitudes is nearly saturated at this time, most of the snowmelt is converted directly into runoff without increasing soil moisture. However, increased absorption of solar energy due to the earlier removal of snow cover during late spring together with the increased absorption of terrestrial radiation mentioned above enhances evaporation from the soil. Therefore, the CO_2-induced increase of evaporation is larger than that of precipitation during late spring and most of the summer as Fig. 14a indicates. On the other hand since both snowmelt and snow cover feedback are absent in PS, evaporation is not increased by these processes. Hence, in high latitudes, the summertime enhancement of the excess of evaporation over precipitation is much less for PS and occurs for a much shorter time than it does for FI, which is consistent with the smaller soil moisture decrease shown in Fig. 13b. These results confirm this conclusion, which was reached in earlier studies such as (Manabe et al. 1981) and (Manabe and Wetherald 1987).

Similar mechanisms also operate in middle latitudes, but their contribution to midlatitude summer dryness is relatively small as indicated by Figs. 2b and 13a,b. Although the change of soil moisture in middle latitudes for PS is both slightly smaller and delayed as compared with FI, the overall amount and timing of soil moisture reduction there for PS is quite comparable to that of FI. This implies that the snow feedback processes play a relatively minor role in enhancing the drying of the soil in middle latitudes during the summer. Because there is much less snow in middle than in high latitudes, the effect of the earlier disappearance of snow followed by enhanced evaporation is considerably reduced there. This is verified by noting that the increases of evaporation over precipitation during late spring and early summer for PS are quite similar to those for FI (Fig. 9a), which suggests that approximately the same degree of soil moisture depletion should occur during the summertime for PS. Therefore, the mechanisms for initiating and enhancing summer dryness in middle latitudes through soil moisture feedback, which were de-

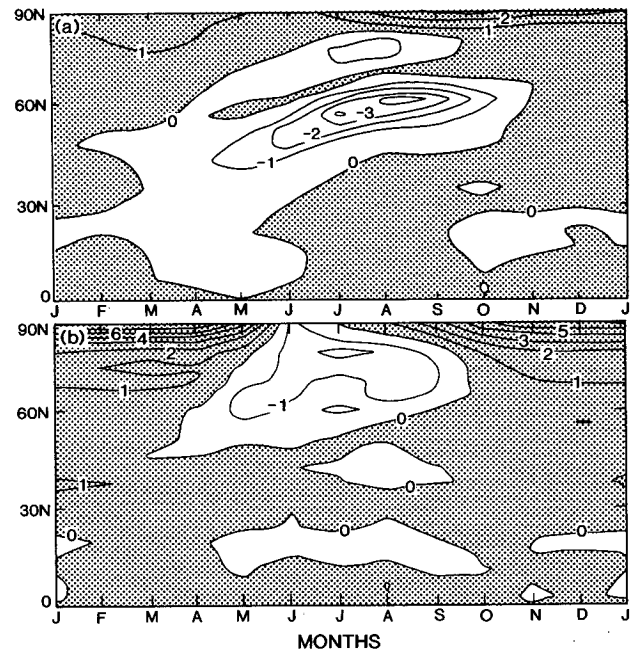

FIG. 13. Latitude–month distributions of zonally averaged, monthly mean difference of soil moisture between the 4× and 1× integrations obtained from the (a) PS experiment and (b) the difference between the FI and PS experiments. Units are in cm.

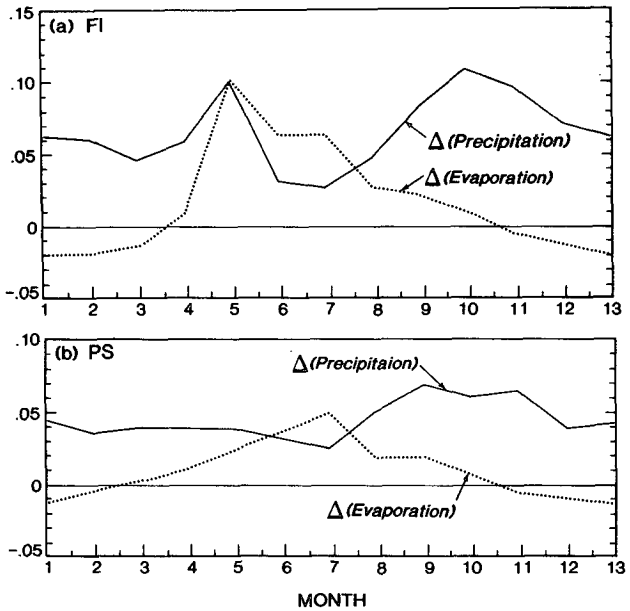

FIG. 14. Seasonal variation of the monthly mean differences of both precipitation and evaporation rates, over the continent, between the 4× and 1× integrations of the (a) FI experiment and (b) PS experiment averaged over the region of 70°–80° lat. Units are in cm day^{-1}. Note that precipitation includes both rainfall and snowfall.

scribed in the preceding section, also apply to the PS experiment.

6. Cloud cover feedback analysis

Another important factor that contributes to the summertime reduction of soil moisture is cloud feedback. This mechanism may be evaluated by comparing the results of the prescribed cloud experiment (PC) with those of FI. In particular, the CO_2-induced change of soil moisture obtained from PC is shown in Fig. 15a, and the difference in soil moisture change between the FI and PC experiments is given in Fig. 15b. According to Fig. 15a, soil moisture is reduced somewhat during the summertime for both middle and high latitudes despite the absence of cloud feedback. However, an examination of Fig. 15b (or both Figs. 2b and 15a) reveals that the summertime reduction of soil moisture is considerably greater for FI than it is for PC. These results indicate that cloud feedback is not necessary to produce summer dryness but, rather, acts to enhance it.

Before proceeding further with the comparison between the PC and FI experiments, it is worthwhile to briefly analyze the interaction between the CO_2-induced changes of low-level relative humidity and cloud cover for the FI experiment as is done in Fig. 16a,b. According to Fig. 16a, low-level relative humidity is reduced substantially during the summer months in the 45°–60° lat region and is accompanied by a similar reduction in total cloud amount (Fig. 16b).

The role of cloud feedback in the summertime reduction of soil moisture may be illustrated by Figs. 17a–e, which show the annual march of the CO_2-induced changes of (a) low-level relative humidity, (b) total cloud cover, (c) absorbed surface insolation, (d) evaporation, and (e) precipitation, respectively, that occur in the 45°–60° lat region for both the FI and PC experiments. These figures indicate that, for the FI experiment (solid lines), the reduction of soil moisture in late spring and early summer results in a significant decrease of both low-level relative humidity (Fig. 16a) and total cloud cover (Fig. 16b) during the summer season. The reduction of cloud cover, in turn, causes a substantial increase of solar radiation absorbed by the land surface throughout the entire summer (Fig. 17c). This additional thermal energy enhances evaporation from the soil surface during early summer (Fig. 17d, June), thereby drying the soil still further. By midsummer, the soil moisture has been reduced in FI to the point where it can no longer support increased evaporation and, therefore, evaporation decreases for the rest of the season (Fig. 17d, July–August). This, in turn, decreases the low-level relative humidity and cloud cover even more causing a corresponding reduction in precipitation over the same period (Fig. 17e). These processes act together to maintain the soil moisture at a lower level throughout the rest of the summer. This is in contrast to the situation for PC (dashed lines) where there is no change of cloud cover and, therefore,

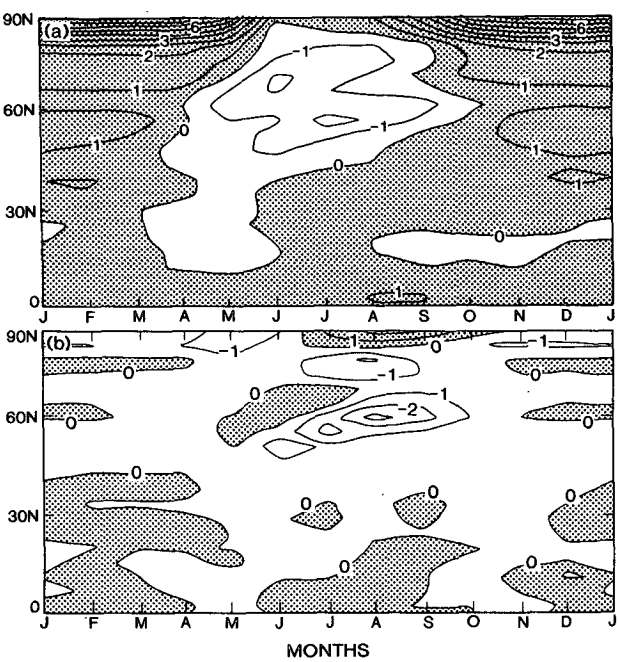

FIG. 15. Latitude–month distributions of zonally averaged, monthly mean difference of soil moisture between the 4× and 1× integrations obtained from the (a) PC experiment and (b) the difference between the FI and PC experiments. Units are in cm.

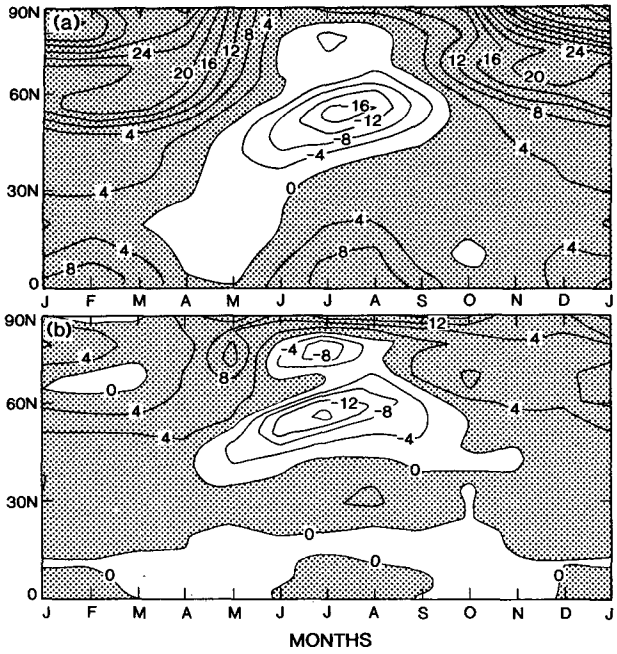

FIG. 16. Latitude–month distribution of zonally averaged, monthly mean difference of (a) relative humidity at the lowest computational level at 991 mb and (b) total cloud amount, over the continent, between the 4× and 1× integrations of the FI experiment. Units are in percent (%).

the absorbed surface insolation actually decreases slightly rather than increases during the summer (Fig. 17c). Because of this, evaporation is not enhanced as much during June for PC as it is for FI (Fig. 17d), which results in less of a reduction of soil moisture for the entire summer for the PC experiment.

These results, taken together, indicate that cloud feedback acts to amplify the reduction of soil moisture in middle latitudes by a decrease of total cloud cover and an increase of absorbed surface insolation, which enhances evaporation during early summer. Although not explicitly discussed, the above conclusion applies to high latitudes as well.

7. Summary and conclusions

In order to identify and elucidate the mechanisms responsible for CO_2-induced summer dryness, several integrations were performed using a R15 version of a GCM with idealized geography. Four separate experiments were conducted: fully interactive model, prescribed soil moisture, prescribed snow cover, and prescribed cloud cover. The response to a quadrupling of CO_2 by each version of the model was then determined and evaluated.

According to the present study, reduction of soil moisture in middle latitudes begins in late spring and is caused by increases of the excess of evaporation over precipitation. The increase of carbon dioxide and the associated increase of atmospheric water vapor enhances the downward flux of terrestrial radiation at the continental surface at all latitudes. However, due mainly to the fact that the midtropospheric relative humidity is reduced in the middle-latitude rain belt and increases slightly in the subtropics, the downward flux of terrestrial radiation increases from 60° to 30° lat, making more energy available for both sensible and

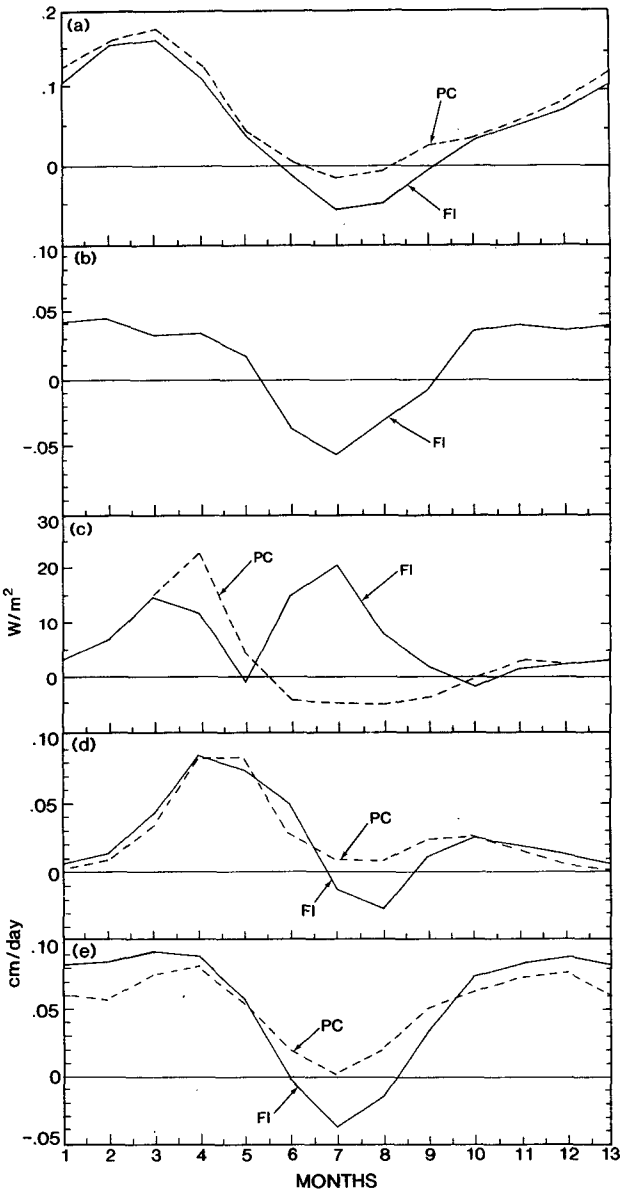

FIG. 17. Seasonal variation of the monthly mean difference between the 4× and 1× integrations of both the FI and PC experiments averaged over the continental region of 45°–60° lat for (a) relative humidity at the lowest computational level at 991 mb, (b) total cloud cover, (c) insolation absorbed by the model surface, (d) evaporation and (e) precipitation. Units are fractions for (a) and (b), W m^{-2} for (c), and cm day^{-1} for both (d) and (e). Here, solid and dashed lines denote results from the FI and PC experiments, respectively.

latent heat in the equatorward side than the poleward side of the middle-latitude rain belt. Since the saturation vapor pressure at the surface increases nonlinearly with surface temperature, a greater portion of the additional radiative energy is realized as latent heat flux at the expense of sensible heat. Therefore, evaporation increases more than precipitation over the land surface in the equatorward side of the middle-latitude rain belt or in the 45°–60° lat region during late spring and early summer and initiates the drying of the soil surface there. As the rain belt moves poleward from spring to summer, the soil moisture decreases in middle latitudes, reducing the rate of evaporation. This, in turn, causes a corresponding decrease of precipitation during summer there and results in a poleward shift of the middle-latitude rain belt keeping the soil dry throughout the summer. These factors all combine to maintain the lower level of soil moisture throughout the entire summer season over continental regions in middle latitudes. However, snow cover/albedo feedback was found to be a relatively insignificant factor in affecting either the timing or the magnitude of midlatitude summer dryness due to the dominance of the mechanisms described above.

The changes of latent and sensible heat are quite different during the winter season in middle latitudes as compared with those during summer. Since the saturation vapor pressure is a nonlinear function of temperature, CO_2-induced increases of latent heat are much less during winter than they are during summer due to the colder surface conditions. Therefore, a greater fraction of the additional radiative energy available at the surface is realized as sensible heat rather than latent heat. Thus, evaporation increases less than precipitation over the continents, thereby contributing to an increase of soil moisture. Precipitation over the continents is also enhanced during winter by increased evaporation from the oceans upstream where the surface temperature is higher than the adjacent continental regions and the additional radiative energy available at the surface is removed more in the form of latent than sensible heat in winter. One should note, however, that the increase of soil moisture is limited in winter because the soil is nearly saturated with water over much of the continents and most of the additional moisture runs off.

In the latitude region of 70°–80°, there is also a tendency for increased summer dryness although it is not as intense as it is in middle latitudes. As noted in our previous studies, this drying is caused, primarily, by an earlier removal of snow cover with a corresponding increase of evaporation during spring, which lengthens the drying period there during the summer. Therefore, snow cover feedback was found to be the dominating mechanism for summer dryness in high latitudes.

Finally, a comparison of the integrations with and without cloud prediction reveals that, while the CO_2-induced reduction of soil moisture occurs during summer despite the absence of cloud feedback, cloud plays a major role in enhancing this dryness. As soil moisture decreases in summer, relative humidity and cloud cover are reduced in the lower model troposphere, contributing to the increase of solar radiation reaching the continental surface. The increase in the surface absorption of radiative energy further enhances the drying by increased evaporation during early summer followed by decreased evaporation and precipitation for the rest of the summer.

As stated in the introduction, several recent GCM investigations conducted with higher-resolution models have yielded the tendency for midlatitude summer dryness obtained by previous GFDL studies with low-resolution models (Mitchell et al. 1990). Similar results were also obtained from the latest combined air–sea transient experiment at GFDL (Manabe et al. 1992). In fact, the only GCM studies that have not produced middle-latitude summer dryness so far are those in which unrealistically dry soil conditions were realized during summer in the control integration, and, therefore, the CO_2-induced increase in evaporation did not exceed that of precipitation, failing to cause further drying of the soil (Meehl and Washington 1988, 1990; Rind et al. 1990). In short, the processes described here occur in a given GCM provided that there is enough soil moisture in the model "buckets" during the summer season in the control integration to allow significant depletions of soil moisture.

As discussed already, the midlatitude continental summer dryness and associated change in precipitation results, essentially, from the CO_2-induced increase in evaporation in late spring and early summer. Therefore, it is not likely that the existence of sharply defined rain belts is a necessary condition for the occurrence of summer dryness.

In assessing the present results, one should recognize that the GCM used here employs a simple "bucket model" parameterization of land surface processes. Because of this simplified formulation, it is possible that the midlatitude continental summer dryness discussed in this study may not be realized in the actual climate system. On the other hand, the simplifications used in this model have facilitated the interpretation of the results from the numerical experiments and the elucidation of the processes involved in the mechanisms of summer dryness. Obviously, the conclusions obtained in this investigation should be reexamined by the use of a GCM incorporating a more realistic parameterization of land surface processes.

Acknowledgments. The authors would like to thank A. J. Broccoli and P. C. D. Milly, as well as two unknown reviewers, for their helpful and constructive comments, which greatly improved the manuscript.

REFERENCES

Bryan, K., 1969: Climate and ocean circulation. Part II: The ocean model. *Mon. Wea. Rev.*, **97**, 828–829.

Gordon, C. T., and W. F. Stern, 1982: A description of the GFDL global spectral model. *Mon. Wea. Rev.*, **110,** 625–644.

Kellogg, W. W., and Z.-C. Zhao, 1988: Sensitivity of soil moisture to doubling of carbon dioxide in climate model experiments. Part I: North America. *J. Climate,* **1,** 348–366.

Manabe, S., 1969: Climate and ocean circulation. Part I: The atmospheric circulation and the hydrology of the earth's surface. *Mon. Wea. Rev.*, **97,** 739–774.

——, and R. T. Wetherald, 1985: CO_2 and hydrology in "Issues in Atmospheric and Oceanic Modeling." *Advances in Geophysics,* Vol. 28, Part A, Academic Press, 131–157.

——, and ——, 1987: Large-scale changes of soil wetness induced by an increase in atmospheric carbon dioxide. *J. Atmos. Sci.,* **44,** 1211–1235.

——, J. Smagorinsky, and R. F. Strickler, 1965: Simulated climatology of a general circulation model with a hydrologic cycle. *Mon. Wea. Rev.*, **93,** 769–798.

——, R. T. Wetherald, and R. J. Stouffer, 1981: Summer dryness due to an increase of atmospheric CO_2 concentration. *Clim. Change,* **3,** 347–386.

——, R. J. Stouffer, M. J. Spelman, and K. Bryan, 1991: Transient responses of a coupled ocean–atmosphere model to gradual changes of atmospheric CO_2. Part I: Annual mean response. *J. Climate,* **4,** 785–818.

——, M. J. Spelman, and R. J. Stouffer, 1992: Transient responses of a coupled ocean–atmosphere model to gradual changes of atmospheric CO_2. Part II: Seasonal response. *J. Climate,* **5,** 105–126.

Meehl, G. A., and W. M. Washington, 1988: A comparison of soil-moisture sensitivity in two global climate models. *J. Atmos. Sci.,* **45,** 1476–1492.

——, and ——, 1990: CO_2 climate sensitivity and snow-sea-ice albedo parameterization in an atmospheric GCM coupled to a mixed-layer ocean model. *Clim. Change,* **16,** 283–306.

Mitchell, J. F. B., and D. A. Warrilow, 1987: Summer dryness in northern mid-latitudes due to increased CO_2. *Nature,* **330,** 238–240.

——, S. Manabe, V. Meleshko, and T. Tokioka, 1990: Equilibrium climate change and its implications for the future. *Climate Change: IPCC Scientific Assessment,* J. T. Houghton, G. J. Jenkins, and J. J. Ephraums, Eds., Cambridge University Press, 131–164.

Posey, J. W., and P. F. Clapp, 1964: Global distributions of normal surface albedo. *Geofis. Int.,* **4,** 33–48.

Rind, D., R. Goldberg, J. Hansen, C. Rosenzweig, and R. Ruedy, 1990: Potential evapotranspiration and the likelihood of future drought. *J. Geophys. Res.*, **95,** 9983–10 004.

Wetherald, R. T., and S. Manabe, 1988: Cloud feedback processes in a general circulation model. *J. Atmos. Sci.,* **45,** 1397–1415.